

# A Golden Section Search Assisted Incremental Conductance MPPT Control for PV Fed Water Pump

Hamza Alrajoubi\*, Selim Oncu\*\*

Department of Electrical & Electronics Engineering, Karabuk University, Karabuk, Turkiye

(hamzaalrajoubi@ogrenci.karabuk.edu.tr, soncu@karabuk.edu.tr)

‡ Corresponding Author; hamzaalrajoubi@ogrenci.karabuk.edu.tr

*Received: 26.05.2022 Accepted: 01.09.2022*

**Abstract-** One way to enhance the effectiveness of photovoltaic (PV) fed water pumping applications is to maximize the solar PV energy by using a suitable design with accurate and fast maximum power point tracking (MPPT). This paper presents a new hybrid MPPT method to improve speed response and efficiency. The method is designed to control a simple standalone PV water pumping system-based single-stage brushless DC (BLDC) motor. A DC-DC converter is eliminated to improve system efficiency and reduce cost. In addition, a two-mode hybrid MPPT algorithm that incorporates the golden-section search (GSS) technique-based MPPT algorithm with incremental conductance (INC) is implemented to enhance the global efficiency of the system. The GSS optimization method handles the initial stages to converge the global peak and helps to increase the convergence rate. In contrast, the INC MPPT method achieves sufficient accuracy with lower oscillation towards the MPPT during the final stages. The designed system is modelled, examined, and compared using traditional techniques in MATLAB/Simulink to evaluate the MPPT efficiency of the model. The results confirm that the proposed MPPT algorithm can successfully drive a 1150W BLDC motor with high tracking efficiency and reliability. The PV energy is transferred to the pump via a voltage source inverter (VSI) using the MPPT algorithm with a proportional-integral (PI) controller. As a result, the MPPT efficiency reached over 99%.

**Keywords** Water pumping system, BLDC motor, hybrid MPPT, GSS.

## 1. Introduction

PV energy has been presented as a hopeful renewable energy source. Due to its benefits in environmental and economic terms [1], it is clean, sustainable and free source, has less maintenance and no noise. The PV panel converts solar energy instantly into electricity [2]. PV energy can be utilized in both standalone applications and grid-connected systems. Among these applications, a standalone PV water pump is an attractive application. It requires a suitable design for solar PV system structure and MPPT control. Using a water storage tank instead of batteries reduces costs and improves efficiency despite its control being more difficult to achieve [3]. Generally, a PV system employs power converter

stages. Its single-stage topology has higher efficiency than the double-stage topology; however, it is more challenging to control. Additionally, its motor efficiency leads to reducing the number of solar PV panels required to generate operating power [4]. Permanent magnet motors have high efficiency. The BLDC motor has an adjustable speed by controlling the input DC voltage, which increases capacity and decreases the system size. Thus, it is a good option, especially in low-power applications [5].

The characteristics of each centrifugal water pump and the PV are the primary issues that need to be addressed to enhance system efficiency [3]. Different MPPT methods are designed to maximize the energy provided by PV arrays. Among the many MPPT methods, the perturb and observe (P&O) and

INC are widely employed to capture the maximum power point (MPP) [6-8]. These can offer several advantages without requiring any previous PV data, including accuracy, simplicity, and robustness, as well as a good response time. According to comparison studies, each of the P&O and INC approaches has a different strategy. The P&O has a high speed for tracking MPP with significant power oscillations at a steady state. It is prone to losing track accuracy if the weather changes rapidly. Although the INC MPPT method has high efficiency with medium tracking speed, its efficiency may be reduced under low-level irradiation [9].

In PV applications, there are multiple methods to handle the situation of the partial shading condition in addition to the MPPT controller to extract the global MPP (GMPP) [10, 11]. Classical MPPT methods are faster than their metaheuristic counterparts, such as genetic algorithms, the grey wolf optimization, the cuckoo search, and the artificial bee colony. In contrast, the metaheuristic methods (random searching) are usually used to locate the GMPP [12, 13]. As a result, tracking the GMPP in the PV water pumping system improves overall operating efficiency [3, 14]. Furthermore, the hybrid MPPT method has been introduced to improve MPPT efficiency [12, 15]. Therefore, some hybrid MPPT methods are presented that integrate the classical and metaheuristic methods to track the global MPP with resistive loads [12, 16].

This study presents a two-mode hybrid MPPT algorithm to control the VSI-supplied BLDC motor-driven water pump. The hybrid algorithm aims to converge the GMPP with high tracking efficiency by combining the GSS-MPPT optimization method and INC MPPT. The operating mechanism of the proposed hybrid algorithm modes depends on atmospheric changes and load conditions. The GSS-MPPT technique handles the initial stages to seek the global peak; it has a high convergence rate and it is robust. Once the MPP is achieved, the algorithm adopts the INC MPPT method. The algorithm mechanism restarts applying the GSS technique whenever it detects changes in weather conditions so as to extract the MPP. As a result, each mode assists the other in enhancing the control reliability and eliminating any adverse effects. The algorithm is designed to help acquire the GMPP and improve the MPPT efficiency and reliability of the system. Thus, the control can meet the requirements of motor drives to track the maximum power of both steady-state and dynamic weather conditions. The proposed hybrid algorithm is modelled and evaluated in MATLAB/Simulink and compared with the classical methods (P&O and INC). The MPPT efficiency and reliability test of the model are compared and presented. The results confirm that the proposed MPPT algorithm can successfully drive the motor with high tracking efficiency and a cost-effective system structure.

## 2. Configuration of the Water-Pump System

Fig. 1 shows the basic design of the PV pump system-based BLDC motor with an MPPT control. A hybrid MPPT method is proposed to control the VSI and enhance efficiency

and reliability in tracking the MPP. The MPPT approach generates the reference voltage, and the error signal feeds the PI controller to acquire the optimum pulse width modulation (PWM). A 1150W BLDC motor loads the VSI with the pump system. This motor has inbuilt hall sensors to provide the rotor position. The correct switching pattern of the PWM is required to drive the VSI switches successfully.

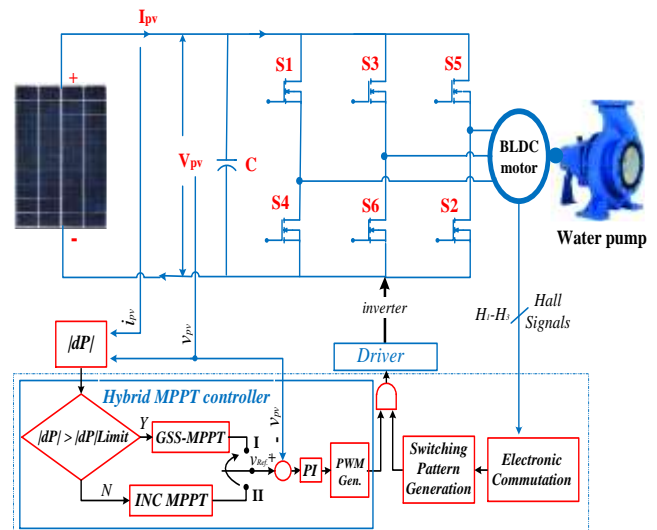


Fig. 1. Water pumping system with the proposed controller

The GSS-INC hybrid-MPPT controller operating principle depends on the limitation value of the PV power change to determine which control mode will be adopted. Mode I utilizes the beneficial features of the GSS-MPPT optimization method, whereas mode II utilizes the features of the INC MPPT approach during the final stages. This hybrid algorithm extracts the MPP with high tracking efficiency and simplicity via the MPPT control.

### 2.1. PV Solar Module

In PV applications, power tracking is necessary to enhance system efficiency [17]. Increasing the PV efficiency leads to an increase in system efficiency [4, 18]. This improvement can be achieved by using the MPPT algorithm, whereas the PV energy is based on available sunlight and temperature. The MPP is a unique operating point on the power-voltage (P-V) curve that requires tracking [9]. This study presents a simple hybrid MPPT method that utilizes instant PV voltage  $v(t)$  and current  $i(t)$  to control the water pumping system. Operating the PV system at an optimal voltage  $v_{MPP}$  value requires the optimum PWM duty ratio. This system utilizes low-power PV array strings, using six PV panels (Soltech 1STH-215-P PV).

### 2.2. Power Inverter Module

According to the maximum power transfer theory, load matching is required to transfer the total PV energy [6]. In PV

systems, it may achieve by generating the reference voltage, which controls the PWM duty ratio of the inverter using the MPPT method. An efficient PV water pump requires a suitable design for the solar PV system structure and MPPT control. Therefore, a single-stage converter with a robust hybrid MPPT controller is applied to enhance system performance. Additionally, trapezoidal control is used to drive the BLDC motor, operating at a 5kHz switching frequency.

### 2.3. BLDC Motor Model

A three-phase brushless DC motor is utilized to rotate the pump. It has inbuilt Hall effect sensors to provide feedback signals of rotor position. By the commutation, a back electromotive force (EMF) is generated in the stator windings. The electromagnetic power ( $P_e$ ) results from multiplying the currents and EMFs, as follows [4]:

$$P_e = i_a e_a + i_b e_b + i_c e_c \tag{1}$$

When the losses are ignored,  $P_e$  can be considered to be [4]:

$$P_e = \tau_e \omega_m \tag{2}$$

where  $\tau_e$  (Nm) is the electromagnetic torque and  $\omega_m$  (rad/s) is the rotor speed.

### 2.4. Water Pump Model

Water pumps are categorized as submersible, surface, and floating pumps according to place of use [3]. The amount of water flowing through a pump is proportional to the speed and torque of the motor although this torque is related to the quadratic speed (in rad/s) [3, 4].

$$\tau_e = K \omega_m^2 \tag{3}$$

Here,  $K$  is the positive constant that is calculated thus [3, 4]:

$$K = \frac{\tau_e}{\omega_m^2} \tag{4}$$

## 3. Proposed Hybrid MPPT Controller

This work presents the development of a new GSS-INC hybrid-MPPT as a fast, accurate, and reliable control to assist in getting the GMPP and improving MPPT efficiency. In addition, applying a single-stage converter for the PV water pump improves overall operating efficiency. The proposed hybrid-MPPT scheme has two modes as shown in Fig. 2. This design aims to acquire the GMPP and improve efficiency by merging the advantages of the GSS-based MPPT and the INC MPPT. Furthermore, the scheme presents these techniques separately to enhance control reliability. The controller block can quickly recognize changes in weather conditions to adopt its operation mode. The proposed MPPT algorithm decides and implements the operation mode of the system according to the actual PV power variation step. A quick response can be generated by using the variation of the power value.

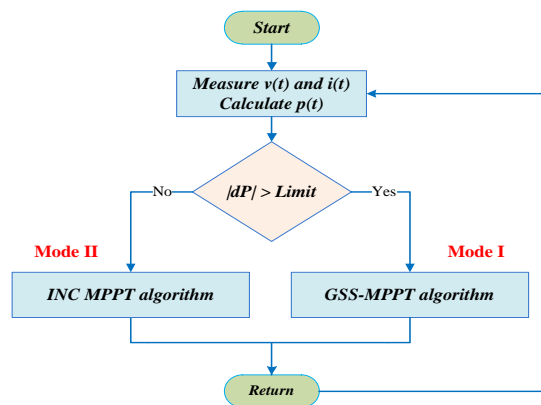


Fig. 2. The proposed hybrid MPPT method

The operation modes depend on atmospheric changes and load conditions. If the weather condition changes, mode I is adopted. Once the MPP is achieved, the algorithm adopts mode II. As a result, mode I handles the initial stages of searching for the global peak, thereby helping to increase the convergence rate. In contrast, mode II achieves an efficiency feature of the INC MPPT approach. Moreover, each mode assists the other in enhancing the control reliability and in eliminating any adverse effects. Therefore, the algorithm can meet the requirements of the motor drives to harvest the MPP of steady-state and dynamic weather conditions.

### 3.1. Golden-Section Search Technique

The American Jack Kiefer was the first to utilize the GSS optimization method to extract the maximum or minimum value of functions within a specified search range. This technique is utilized to support different algorithms in many applications [19]. The golden ratio of a segment length is [20]:

$$\frac{1}{L} = \frac{L}{1-L}, \quad 0 < L < 1 \tag{5}$$

Solving this equation is the golden ratio (GR) of  $(\sqrt{5} - 1)/2$ . The search step size of the golden-section search strategy depends on this ratio. Additionally, multiplying the golden ratio may be used to improve system performance [20]. Although the GSS technique extracts the GMPP and improves the convergence rate [3, 21], its operation mechanism also ensures that the voltage values spread out from each other in tracking the MPP. This technique is robust and noise-resistive because it contains no derivatives. Moreover, it has excellent tolerance for measurement errors of power ripple issued by the switching mode inverter [19, 22].

### 3.2. Principle of the Hybrid MPPT Controller

In the presented hybrid algorithm, the instant PV voltage  $v(t)$  and current  $i(t)$  values are measured and the instant actual power is calculated. The absolute value of instant actual power  $p(t)$  compared to previous power  $p(t - 1)$  is presented as  $|dP|$ , which depends on atmospheric conditions. According

to this comparison, if  $|dP|$  is greater than the limited value of the power oscillation, the GSS-MPPT optimization method (Mode I) control is employed. Otherwise, the INC MPPT method (Mode II) control is adopted during or near the MPP. Therefore, the operating mechanism of the algorithm modes depends on the modified limit value of  $|dP|$  to determine which mode will be adopted. The limit is estimated relying on the rate of the PV power change around the MPP. Once the power oscillations are within this limit, the algorithm switches to mode II, and then waits for the increment of the  $|dP|$  value to initiate mode I again. Fig. 3 shows the operation regions of the presented hybrid method on the PV power characteristic.

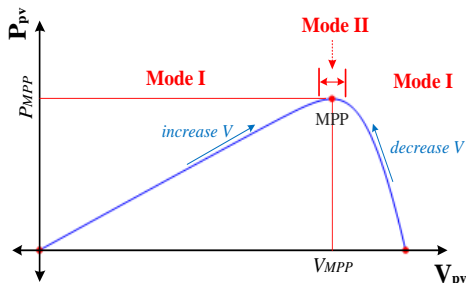


**Fig. 3.** Operation regions of the hybrid MPPT method

It can be observed that the operating principle of the modes depends on the power slope. The power slope ( $dP/dV$ ) in the region of mode II is nearly zero, so the rate of the PV power change  $|dP|$  is low, whereas the rate of the power change in the region of mode I is higher than the rate of the power change in the region of mode II. Therefore, the power limitation can be modified using instant actual PV power change to determine the suitable operation mode. This limit ensures that mode I is activated during transients and varying irradiance, and mode II is activated during steady-state power tracking. A detailed flowchart of the proposed hybrid MPPT method is shown in Fig. 4. In this algorithm, mode I works at the onset and if dynamic atmospheric conditions are detected with high-speed tracking. Once steady-state power is achieved, mode II will automatically engage with a small step size value to avoid power oscillations for maximize efficiency. If the weather condition changes, it will handle mode I again until a steady-state of power is accomplished.

#### A. Operation of Mode I

In Fig. 4, the mode I (GSS-MPPT) flowchart is shown. Mode I is adopted whenever the instant value of  $|dP|$  is greater than the PV power limitation. Hence, mode I estimates the

initial MPP at two conditions, firstly while the system starts up and then while a dynamic weather condition is recognized. This mode generates the reference voltage in dynamic weather conditions by using a rapid tracking feature of the GSS-MPPT technique. In search space optimization, the GSS strategy generates two points that divide the search interval  $[a, b]$  into three sections. Therefore, the two values of reference voltage are given such that [21]:

$$v_1 = a + 0.618 (b - a) \quad (6)$$

$$v_2 = b - 0.618 (b - a) \quad (7)$$

The power values ( $P_1, P_2$ ) of these voltages are measured as in Fig. 4. Then according to the comparison, if  $P_1$  is greater than  $P_2$ , the algorithm eliminates all voltage points that are less than  $v_2$  ( $v < v_2$ ); if  $P_2$  is greater than  $P_1$ , it eliminates all voltage points that are greater than  $v_1$  ( $v > v_1$ ). This process reverts again to shrink the desired tolerance ( $\epsilon$ ) and define the stop iterative. As a result, some iterative processes are required to seek the global MPP in a particular domain of the PV power-voltage curve. Once the maximum power is achieved, the algorithm switches to mode II, then waits for the value increment of  $|dP|$  to initiate mode I again to find the MPP.

#### B. Operation of Mode II

Finally, mode II is used to verify the MPP by detecting and tracking the movement of the MPP at the power steady-state. Therefore, whenever the instant value of  $|dP|$  is within the PV power limitation, the algorithm switches to mode II to work in the final stages. This forces the system to have a fast and accurate track of the MPP with reduced oscillations. As it is known, the INC MPPT method is an accurate way to track the MPP where the power slope is zero ( $dP/dV = 0$ ). As a result, mode II generates the reference voltage using the efficiency feature of the INC MPPT method with a small step size; therefore, oscillations of the PV voltage and power will be reasonably low. In contrast, the PI controller keeps the reference voltage constant when optimum power is achieved, and the system is forced to track the MPP if there is no change in the weather. If mode II recognizes that the optimum power has been lost, mode I will operate again to seek the global MPP. Therefore, if one of the modes fails to track the MPP, the other mode will operate to track it instead in order to enhance the control reliability and eliminate any adverse effects. The algorithm holds the PV water pumping system operating at the global optimum power.

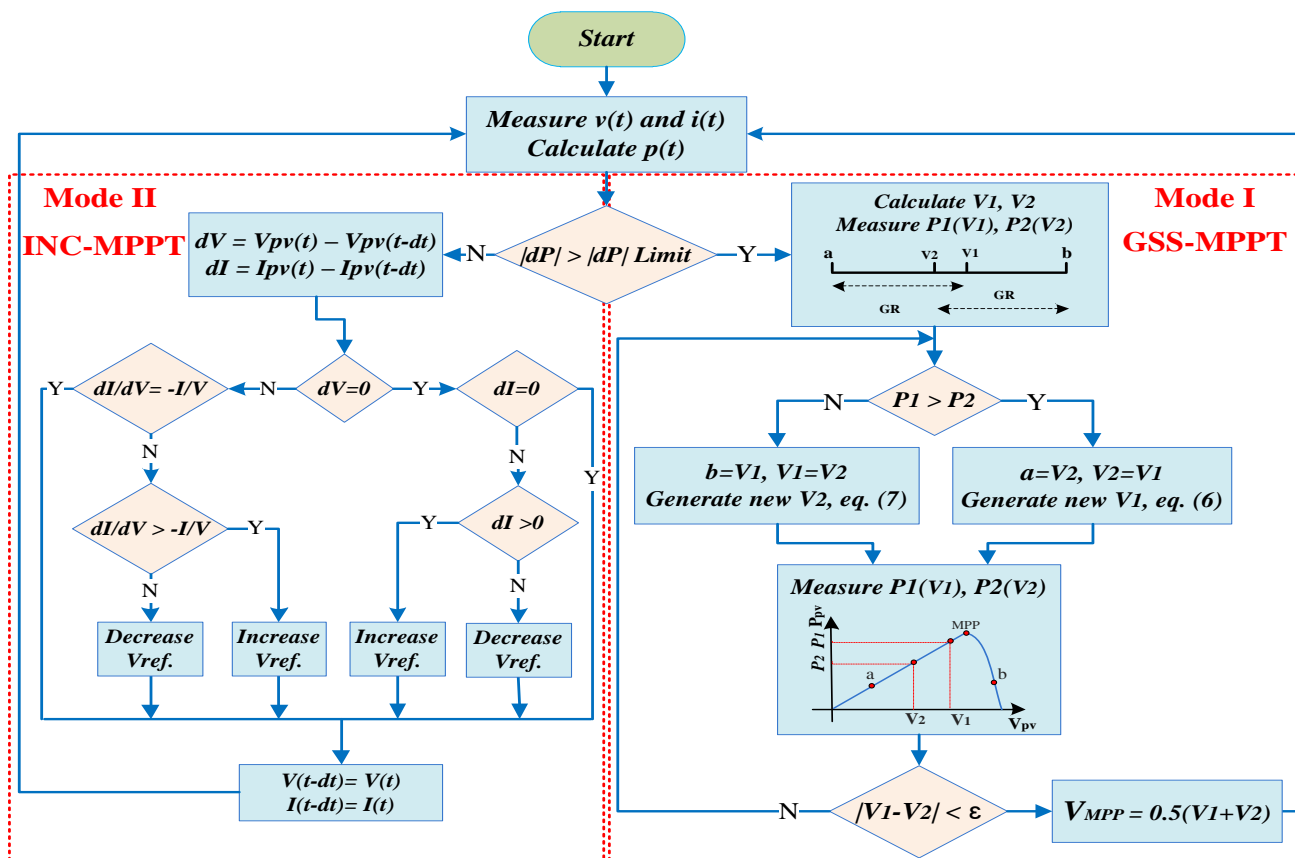


Fig. 4. Detailed flowchart of the proposed hybrid MPPT algorithm with INC and GSS

4. Modelling and Simulation

The presented PV pump system-based BLDC motor with an MPPT controller is modelled in MATLAB/Simulink. The model contains six PV panels that are connected in three parallel branch strings. The specification of the PV panel is selected to be PV power  $p(t)$ , voltage  $v(t)$  and current  $i(t)$  respectively being 213.15 W, 29 V and 7.35 A at the MPP. As a result, the PV panels capacity of the proposed system is 1279 W and its voltage rate is 58 V under standard conditions ( $1000 \text{ W/m}^2$ ,  $25^\circ\text{C}$ ). The PV array feeds a 1150W BLDC motor through the VSI crossing a DC link capacitor. This motor is loaded using the water-pump model. Three Hall sensors generate Hall signals to provide the correct switching pattern. On the other hand, the algorithm generates an optimum value of the reference voltage to compare with the actual PV voltage. Then the error signal feeds the PI controller to give the control signal (duty cycle), which, for reasons of safety, is limited between 0.2 and 1.0. As a result, the PWM signals are generated sequentially to control VSI switches (S1 to S6). The PV solar water-pump system model is examined at three irradiation levels of  $300 \text{ W/m}^2$ ,  $500 \text{ W/m}^2$ , and  $1000 \text{ W/m}^2$  at a temperature of  $25^\circ\text{C}$ . Fig. 5 shows the power-voltage curve of the solar PV panels under three irradiation levels showing the PV optimum values of the voltage  $V_{MPP}$

and maximum power  $P_{MPP}$ . The MPPT efficiency of the GSS-INC hybrid algorithm is evaluated and compared with both classical methods, the P&O and INC methods.

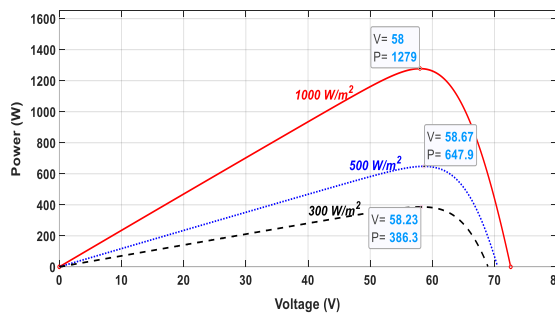


Fig. 5. P-V curve of tested irradiances

5. Results and Discussion

The characteristics of each water pump and the solar PV are the challenges to control, especially when using a single-stage converter. Therefore, it requires a robust MPPT control to extract the GMPP and achieve high tracking efficiency. The model is designed, and the MPP tracking effectiveness is compared with both classical methods (P&O and INC) to verify the efficiency of the enhancement. The MPPT

efficiency of the model is evaluated. Finally, the output power tracking of the system with rapidly changing irradiance levels is tested. The results confirm that the GSS-INC hybrid can successfully drive the motor-pump in steady and dynamic atmospheric conditions with high tracking efficiency.

*A. Comparison with INC MPPT*

The designed model is examined using (hybrid and INC) MPPT controllers to track the MPP for different irradiance levels. Fig. 6 illustrates the result of the output power tracking using the proposed method and the tracked power with the INC MPPT method compared to the reference power. The green line is the PV reference power  $P_{MPP}$ , and the red line the PV output power with the hybrid MPPT controller. In contrast, the black line is the tracked PV power with the INC approach. It can be observed that they are completely identical to what is illustrated in Fig. 6.

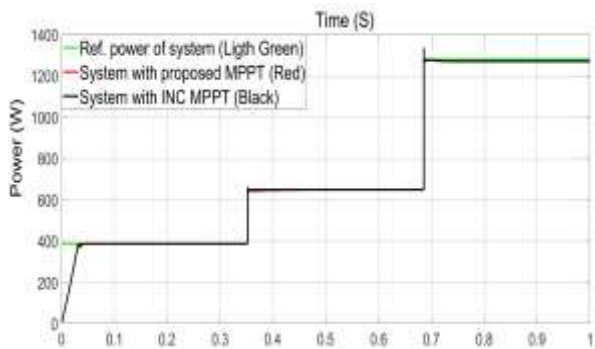


**Fig. 6.** Power tracking with the hybrid and INC MPPT

The result illustrates the high MPP tracking efficiency of the system using the MPPT controller, which can successfully drive a 1150W BLDC motor.

Fig.7 shows the starting response of the tracked PV power with (hybrid and INC) MPPT controllers at irradiation levels of  $300 \text{ W/m}^2$ . The result indicates that the optimum power is reached in 33 ms or less after starting up with the GSS-INC hybrid MPPT controller. Moreover, the output power tracking result confirms that it can quickly track the MPP under rapid atmospheric changes. In contrast, the result indicates that the system reaches the stable maximum power in approximately 43 ms after starting up with the INC MPPT controller.

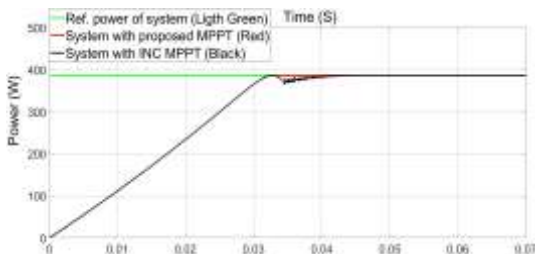


**Fig. 7.** Starting response of the tracked PV power

The result of the tracked PV power oscillations of the system with (hybrid and INC) MPPT controllers are shown in

Fig. 8. The result shows that the power oscillation of the system with the proposed method is around the MPP (647.6 – 648.1 W) in the steady-state regime at irradiation levels of  $500 \text{ W/m}^2$ . As a result, the power oscillation of transient and steady states is reasonably low due to the beneficial feature of the INC MPPT approach with a small step size. In contrast, the result shows that the power oscillation of the system with the classical INC MPPT is around the MPP (646.5 – 648.1 W).

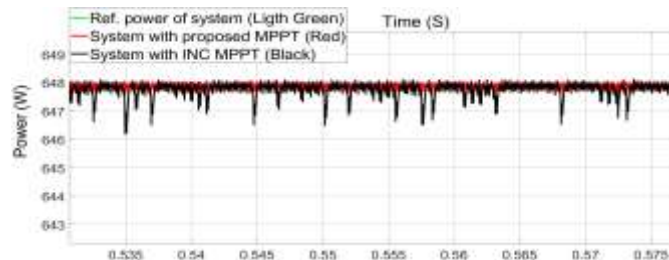


**Fig. 8.** Zoom of steady-state power oscillations at ( $500 \text{ W/m}^2$ )

*B. Comparison with P&O MPPT*

The designed model is examined using (hybrid and P&O) MPPT controllers to track the  $P_{MPP}$  for different irradiance levels. The Fig. 9 shows the output power results for the proposed algorithm and the conventional P&O method. The green line is the PV reference power  $P_{MPP}$ , and the red line the PV output power with the hybrid MPPT controller. In contrast, the blue line is the tracked power with the P&O MPPT.

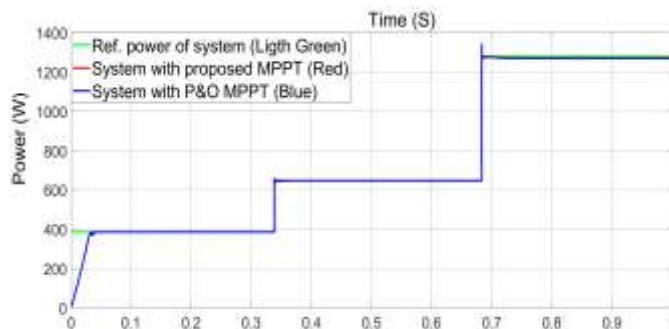


**Fig. 9.** Power tracking with the hybrid and P&O MPPT

Fig.10 shows the starting response of the tracked PV power with (hybrid and P&O) MPPT controls at irradiation levels of  $300 \text{ W/m}^2$ . The result indicates that the system reaches the stable maximum power in approximately 43 ms after starting up with the P&O MPPT controller.

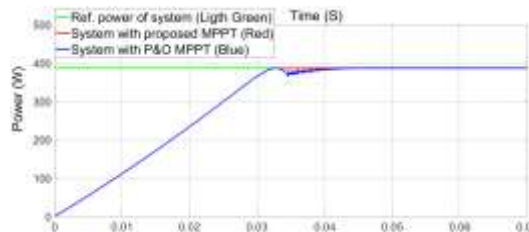


**Fig. 10.** Starting response of the tracked PV power

The power oscillations of the system with (hybrid and P&O) MPPT controls are shown in Fig. 11. The result shows that the power oscillation of the system with the P&O MPPT is around the MPP (645.5 – 648.1 W) in the steady-state regime at irradiation levels of 500 W/m<sup>2</sup>. The steady-state oscillation is primarily affected due to the mechanism of the control method and step size.

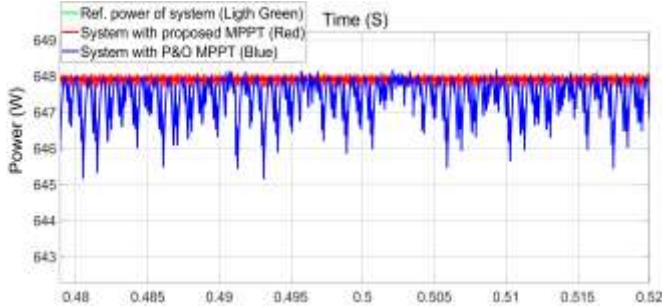


Fig. 11. Zoom of steady-state power oscillation at (500 W/m<sup>2</sup>)

The obtained results verify that the power tracking of the water pumping system with the MPPT controls being used (hybrid, INC, and P&O) can successfully track the P<sub>MPP</sub> for different irradiance levels. The proposed algorithm has high tracking efficiency and reliability, which means robust control of the PV water pumping system-based BLDC motor loaded VSI.

### C. System Response with MPPTs

Fig. 12 shows the motor speed response following the hybrid, INC and P&O methods at three irradiance levels.

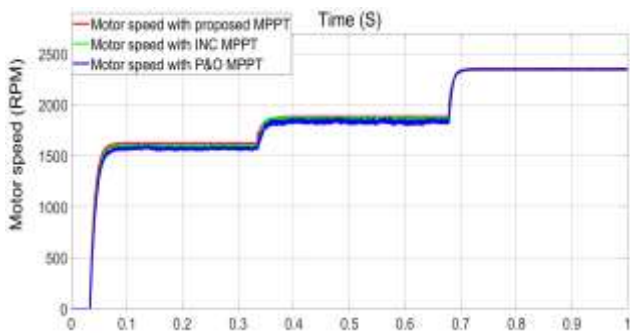


Fig. 12. Motor speed response at three irradiance levels

It can be observed that the speed response is adapted smoothly according to the irradiance level in order to hold the PV pump system at its optimum power. The result illustrates that the motor exhibits an excellent speed response, and the pump operates within a suitable range of speed under different irradiance levels. The pump-speed level exceeds 1600 rpm and the irradiance is 300 W/m<sup>2</sup> under 25 °C.

The pump load response with (hybrid, INC, and P&O) MPPT controls at three irradiance levels is shown in Fig. 13. The pump model is used to load the BLDC motor. This load T<sub>L</sub> (in Nm) is proportional to the square of the motor speed ω<sub>m</sub> (in rad/s).

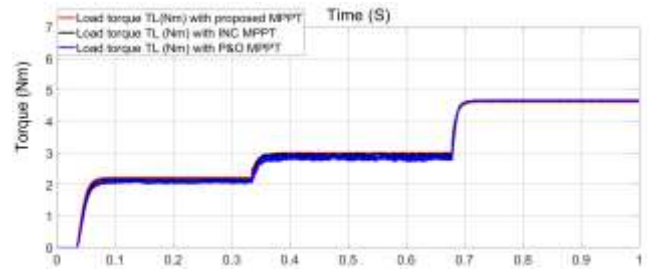


Fig. 13. Pump load response at three irradiance levels

Finally, Fig. 14 shows the generated reference voltage v<sub>ref</sub> using the hybrid MPPT algorithm at three irradiance levels (300, 500, and 1000 W/m<sup>2</sup>) sequentially. Comparing this reference voltage and the actual PV voltage gives an error. This error signal supplies the PI controller the necessary information to determine the optimum PWM duty cycle which forces the water pumping system to operate at the MPP.

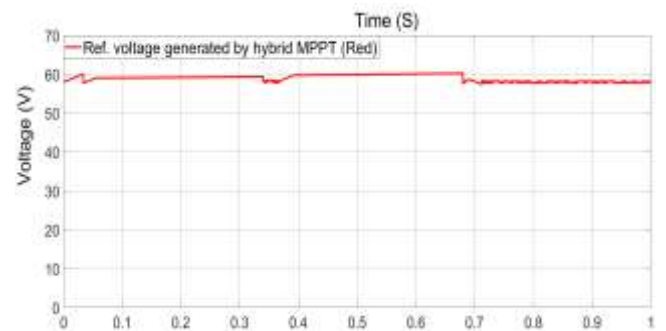


Fig. 14. Generated voltage by the proposed algorithm

The results show that the GSS-INC algorithm updates the reference voltage when there is a change in irradiance level. It can be observed that the generated voltage v<sub>ref</sub> corresponds to the optimum voltage v<sub>MPP</sub> (58.23 V, 58.67 V, and 58.00 V) of the PV array, as shown in Fig. 5. Furthermore, the result of the simulation confirms that the convergence rate of the GSS method is high in each computational iteration reducing the search time. In comparison, it reduces the search interval by 38.2% instead of the fixed step size. A further advantage is that its mechanism searches within the overall specified search interval (left and right of the MPP) helps to find the global MPP with low computation. Since the GSS technique depends on search optimization, extracting and maintaining the GMPP is anticipated.

### D. Hybrid MPPT Efficiency

The proposed hybrid MPPT efficiency (η<sub>MPPT</sub>) can be evaluated using the following equation [9]:

$$\eta_{MPPT} = \frac{P_{out}}{P_{MPP}} \times 100 \% \quad (8)$$

Here, P<sub>MPP</sub> is the theoretical power of the PV modules (reference power) and P<sub>out</sub> is the PV output power. P<sub>out</sub> is evaluated using the actual PV voltage v(t) and current i(t).

**Table 1.** Hybrid MPPT efficiency under different irradiances

S (W/m <sup>2</sup> )	P <sub>MPP</sub> (W)	P <sub>out</sub> (W)	η <sub>MPPT</sub> (%)
100	124.1	123.4	99.44
200	254.8	253.4	99.45
300	386.3	384.5	99.53
400	517.6	515.0	99.50
500	647.9	644.7	99.51
600	777	772.7	99.45
700	904.7	900.3	99.51
800	1031	1025	99.42
900	1155	1150	99.57
1000	1279	1271	99.37

The results confirm that the GSS-INC MPPT algorithm has high tracking efficiency. It offers a number of advantages, including accuracy, simplicity, robustness, and high reliability of the algorithm. It can also be observed that the power tracking efficiency η<sub>MPPT</sub> exceeds 99%.

*E. Reliability Test of Hybrid MPPT Controller*

Here, the model is tested in rapidly changing irradiation levels (200, 300, 500, 700, and 1,000 W/m<sup>2</sup>) under a temperature of 25°C. The irradiation levels are selected to simulate and include shading in the worst case of solar radiation reduction to verify the efficiency of the GSS-INC algorithm. Fig. 15 shows the power tracking of the system with the GSS-INC MPPT control to prove its reliability in rapidly changing weather conditions.

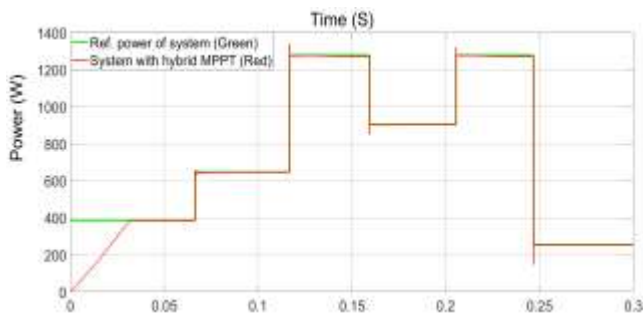


**Fig. 15.** Power tracking of the system with rapidly changing irradiance levels

In Fig. 15, the green line represents the reference power of the PV modules and the red line represents the output power with the hybrid MPPT controller. The obtained results confirm that the PV water pump system with the GSS-INC MPPT algorithm enhances the global efficiency of the system and its reliability. The results verify that the algorithm is a robust control for the single-stage PV-supplied water pump.

**6. Conclusion**

This paper presents an efficient and reliable PV water pumping system based BLDC motor controller by a novel hybrid MPPT algorithm. The hybrid MPPT design aims to combine the features of the GSS-based MPPT strategy and INC MPPT algorithm. The power limitation is modified to ensure that the algorithm extracts the MPP of both steady-state and dynamic weather conditions. Therefore, the algorithm applies the GSS technique whenever the controller recognizes that weather conditions change. Moreover, each mode supports the other to enhance the control reliability and eliminate any adverse effects. The algorithm yields high MPP tracking efficiency and low power oscillations. The proposed hybrid MPPT design concept may be used to incorporate other MPPT method features. The designed system has been implemented in MATLAB/Simulink and compared with conventional P&O and INC approaches. Simulation results illustrate that the designed model with the proposed hybrid MPPT control can successfully drive a 1150W BLDC motor. The proposed system can reach the maximum power in 33 ms or less after starting, reaching the MPP more quickly under rapid atmospheric changes. The power tracking oscillation found approximately 0.5W in the steady state regime. The hybrid MPPT efficiency is obtained over 99%.

**References**

- [1] A. Karafil, H. Ozbay, and S. Oncu, "Design and Analysis of Single-Phase Grid-Tied Inverter with PDM MPPT-Controlled Converter", IEEE Transactions on Power Electronics, Vol. 35, No. 5, pp. 4756-4766, May 2020.
- [2] H. Sher, A. Rizvi, K. Addoweesh, and K. Al-haddad, "A Single Stage Stand-Alone Photovoltaic Energy System (SAPES) with High Tracking Efficiency", IEEE Trans. on Sustain. Energy, Vol. 8, No. 5, pp. 755-762, April 2017.
- [3] S. Djeriou, A. Kheldoun, and A. Mellit, "Efficiency Improvement in Induction Motor-Driven Solar Water Pumping System Using Golden Section Search Algorithm" Springer, Arab. J. Sci. Eng., vol. 43, pp. 3199-3211, June 2018.
- [4] H. Alrajoubi, S. Oncu, and S. Kivrak, "An MPPT Controlled BLDC Motor Driven Water Pumping System", 10th International Conference on Renewable Energy Research and Application (ICRERA), Istanbul, pp. 116-119, 26-29 September 2021.
- [5] R. Kumar and B. Singh, "Single Stage Solar PV Fed Brushless DC Motor Driven Water Pump", IEEE Journal of Emerging and Selected Topics in Power Electronics, Vol. 5, No. 3, pp. 1377-1385, September 2017.
- [6] H. Rezk and A. Eltamaly, "A comprehensive comparison of different MPPT techniques for photovoltaic systems", Sol. Energy, vol. 112, pp. 1-11, February 2015.
- [7] H. Ozbay, A. Karafil, S. Oncu, and M. Kesler, "PSIM Simulation of Flyback Converter for P&O and IC MPPT

- Algorithms”, *European Journal of Engineering and Natural Sciences (EJENS)*, Vol. 2, No. 1, pp. 204-209, 2017.
- [8] A. Belkaid, I. Colak, K. Kayisli, and R. Bayindir, “Improving PV System Performance using High Efficiency Fuzzy Logic Control”, 8th International Conference on Smart Grid (icSmartGrid), Paris, pp. 152-156, 17-19 June 2020.
- [9] N. Bizon, N. Mahdavi, F. Blaabjerg, and E. Kurt, *Energy Harvesting and Energy Efficiency*, Springer, vol. 37. Switzerland Press, 2017, Lecture Notes in Energy.
- [10] S. Xu, R. Shao, B. Cao, and L. Chang, “Single-phase Grid-connected PV System with Golden Section Search-based MPPT Algorithm”, *Chinese Journal of Electrical Eng.*, Vol. 7, No. 4, pp. 25-36, December 2021.
- [11] B. Veerasamy, T. Takeshita, A. Jote, and T. Mekonnen, “Mismatch Loss Analysis of PV Array Configurations under Partial Shading Conditions”, 7th International Conference on Renewable Energy Research and Appl. (ICRERA), Paris, pp. 1162-1183, 14-17 October 2018.
- [12] M. Kermadi, Z. Salam, J. Ahmed, and E. M. Berkouk, “An Effective Hybrid Maximum Power Point Tracker of Photovoltaic Arrays for Complex Partial Shading Conditions”, *IEEE Trans. on Indus. Elec.*, Vol. 66, No. 9, pp. 6990-7000, September 2019.
- [13] M. Kermadi and M. Berkouk, “Artificial intelligence-based maximum power point tracking controllers for Photovoltaic systems: Comparative study”, *Renew. and Sustain. Ene. Reviews*, vol. 69, pp. 369-386, March 2017.
- [14] A. Lakhdera, T. Bahi, and A. Moussaoui, “Performance of Pumping System Under Partial Shading”, *IEEE 2nd International Maghreb Meeting of the Conference on Sciences and Techniques of Automatic Control and Computer Engineering (MI-STA)*, Libya, pp. 686-691, 23-25 May 2022.
- [15] H. Sher, K. Addoweesh, and K. Al-Haddad, “An Efficient and Cost-Effective Hybrid MPPT Method for a Photovoltaic Flyback Microinverter”, *IEEE Trans. on Sustain. Energy*, Vol. 9, No. 3, pp. 1137-1144, July 2018.
- [16] A. Farayola, Y. Sun and A. Ali, “ANN-PSO Optimization of PV Systems Under Different Weather Conditions”, 7th International Conference on Renewable Energy Research and Application (ICRERA), Paris, pp. 1363-1368, 14-17 October 2018.
- [17] A. Nusaif, and A. Mahmood, “MPPT Algorithms (PSO, FA, and MFA) for PV System Under Partial Shading Condition, Case Study: BTS in Algazalia, Baghdad”, *International Journal of Smart grid*, Vol. 10, No. 3, pp. 100-110, September 2020.
- [18] A. Issa and Z. Yusupov, “Development of a Mas Based Distributed Intelligent Control and Fault Control Strategy for Microgrid”, *Polyteknik Dergisi*, Vol. 24, No. 1, pp. 161-173, 2021.
- [19] I. Yazıcı, E. K. Yaylacı, and F. Yalçın “Modified golden section search based MPPT algorithm for the WECS”, *Eng. Science and Technology an International Journal*, Vol. 24, No. 4, pp. 1123-1133, October 2021.
- [20] F. Silva, R. Borries, and C. Miosso, “Golden number sampling applied to compressive sensing”, *IEEE Southwest Symposium on Image Analysis and Interpretation (SSIAI)*, Las Vegas: USA, 08-10 April 2018.
- [21] A. Kheldoun, R. Bradai, R. Boukenoui, and A. Mellit, “A new Golden Section method-based maximum power point tracking algorithm for photovoltaic systems”, *Energy Convers. and Manag.*, vol. 111, pp. 125-136, March 2016.
- [22] R. Shao, R. Wei, and L. Chang, “A multi-stage MPPT algorithm for PV systems based on golden section search method”, *IEEE Applied Power Electronics Conference and Exposition - APEC*, Fort Worth: USA, 16-20 March 2014.